IEEE Access
Multidisciplinary | Rapid Review | Open Access Journal

Received January 25, 2020, accepted February 16, 2020, date of publication February 24, 2020, date of current version March 3, 2020.

Digital Object Identifier 10.1109/ACCESS.2020.2975990

Stochastic MPC-Based Air-Fuel Ratio Regulation of Compressed Natural Gas Engines

JUN YANG[1,2] **AND BO SUN**[1]
[1]Department of Control Science and Engineering, Shandong University, Jinan 250061, China
[2]Department of Automotive Engineering, Shandong Jiaotong University, Jinan 250357, China

Corresponding author: Bo Sun (sunbo@sdu.edu.cn)

This work was supported by the National Natural Science Foundation of China under Grant 61733010, Grant 61821004, and Grant 61803231.

ABSTRACT In this paper, the air-fuel ratio regulation problem of compressed natural gas (CNG) engines is considered by employing stochastic model predictive control (MPC) technology. A stochastic model predictive regulator based on a discrete-time dynamic model of CNG engines is proposed, taking into account the residual gas, and the closed-loop system is deduced to be stochastically stable. A numerical simulation is performed to demonstrate the effectiveness of the proposed control scheme under two working conditions. The simulation results show that the performance of the proposed stochastic model predictive regulator is better than that of the open-loop controller.

INDEX TERMS Stochastic model predictive control, air-fuel ratio regulation, compressed natural gas engines.

I. INTRODUCTION

Natural gas is a widely acknowledged apposite alternative fuel that can help improve the environment and address energy issues, owing to its widespread distribution, clean-burning properties and higher proportion of hydrogen to carbon [1]. Consequently, natural gas engines have received considerable attention to realize fuel saving and reduce emissions.

The air-fuel ratio in the pre-combustion chamber of CNG engines, corresponding to various mixtures and fuel flow rates can be estimated using a model established in [2]. The emission and combustion performance of a natural gas engine with excess hydrogen, which is affected by the compression ratio under diverse air-fuel ratios has been described in [3]. The influence of the components of natural gas on the combustion and emission performance of natural gas engines has been researched, and the well-known results in this research domain has been reported in [4]. In [5], researchers investigated the particle emission characteristics of natural gas engines operating a traditional oil fueled engine with natural gas. The cyclic variation of the combustion in a pre-mixed natural gas engine with the mixture characteristics was investigated in [6]. In [7], the researchers performed experiments to improve the combustion efficiency of natural gas engines enhancing the compression ratio to achieve a larger expansion ratio. In [8], to clarify the potential of CNG for transport applications, an experimental investigation of the laser ignition of a mixture of lean CNG and air under various compression ratios and excess air ratios has been expressed. The results of recent research pertaining to the performance of CNG engines in terms of the power, efficiency, and other factors have been provided in [9]. In [10], the combustion and emission performance of a CNG engine using a stratified air-fuel mixture were investigated, and overall engine efficiency was improved compared to that of the premixed type engine. To clarify the content of methane, the technology of fuel adaptive injection of CNG engines was investigated in [11]. A reduced order dynamic model of twin spool gas turbine was established for the tracking problem in [12], and a sliding mode controller was designed based on the theory of finite-time stabilization, e. g. [13]. To reduce the root and carbon dioxide emissions of diesel engines, performances of CNG engines with different replacement rates were compared in [14], and the hole size of the fuel injector was optimized. However, the fuel economy and emissions of CNG engines are considerably affected by the control accuracy of the air-fuel ratio. In practice, the performance of the air-fuel ratio control is affected by many factors, such as the so-called residual gas trapped in the cylinder at the end of the exhaust stroke, which reflects stochastic characteristics. Moreover, the inaccuracy of the dynamic models of CNG engines also

The associate editor coordinating the review of this manuscript and approving it for publication was Juntao Fei.

considerably influences the control accuracy of the air-fuel ratio. An intuitive approach to solve the above problems is to employ the stochastic MPC technology, using which, the limitations of the stochasticity of the residual gas and inaccuracy of the dynamic model can be overcome.

Consequently, the stochastic MPC technology has been widely researched and applied to several practical systems. In [15], the researchers developed a control algorithm to enable the operation of an energy vehicle by combining stochastic MPC with learning, and the proposed control algorithm was validated by considering the energy distribution of a hybrid electrical vehicle. An energy distribution algorithm based on the stochastic MPC theory was developed in [16], by considering the vehicle allocation, driving direction, and transportation information of hybrid electrical vehicles operating in hilly areas with less traffic. A stratified stochastic control algorithm for the energy management of charging of plug-in electrical vehicles and wind energy in a micro-grid was presented in [17], to enable the coordination of plug-in electric vehicles and wind energy. The use of restriction fastening to anti conservatively ensure the stability and recursive practicability in a stochastic MPC was reported in [18]. In [19], the framework of a stochastic MPC is described in context of a certain real-time permission regarding the regulation of the energy and frequency markets for an immobilization battery. Considering the energy distribution of micro-grids involving double glazed units, a control algorithm combined with the MPC working under two different time axes was proposed in [20].

In this paper, the regulation problem of the air-fuel ratio of CNG engines is addressed by using a stochastic MPC algorithm based on the air path and fuel path dynamics. The stochasticity of residual gas is modelled as a Markov chain [21], and the stabilization of the whole system is considered. The control accuracy of the air-fuel ratio is improved, since the statistical information of the residual gas transitions is fully utilized, and the influence of the inaccuracy of the dynamic model is eliminated by using a stochastic model predictive regulator. A numerical simulation is performed to demonstrate the effectiveness of the employed air-fuel ratio stochastic model predictive regulator.

II. STOCHASTIC MPC ALGORITHM DESIGN

The stochastic air-fuel ratio regulator is designed as described in this section. Because the dynamics of CNG engines is the same as that of gasoline engines, a model of gasoline engines, which involves the air path and fuel path dynamics, as established in [21], is used:

$$\begin{aligned} M_a(k+1) &= \left(M_a(k) - \lambda_d \mu M_f(k)\right) r(k) + M_{an}(k), \\ M_f(k+1) &= M_f(k)(1-\mu) r(k) + M_{fn}(k), \end{aligned} \tag{1}$$

where $M_a(k)$ denotes the mass of the total air in the cylinder, $M_f(k)$ denotes the mass of the total fuel in the cylinder, λ_d denotes the ideal air-fuel ratio, $\mu \in (0,1)$ denotes the efficiency of combustion, $M_{an}(k)$ denotes the mass of fresh air, and $M_{fn}(k)$ denotes the mass of fresh fuel, $r(k)$ denotes the residual gas fraction, and is considered as a finite-state irreducible aperiodic Markov chain whose state space S and one-step transition probability matrix P can be expressed as follows:

$$S = \{s_1, \cdots, s_n\}, \tag{2}$$

and

$$P = \begin{pmatrix} p_{11} & \cdots & p_{1n} \\ \vdots & \ddots & \vdots \\ p_{n1} & \cdots & p_{nn} \end{pmatrix}, \tag{3}$$

where s_i denotes the state, and p_{ij} denotes the one-step transition probability. The error of regulation of the air-fuel ratio $y(k)$ is defined as

$$y(k) = M_a(k) - \lambda_d M_f(k). \tag{4}$$

Rearranging system (1) and (4) yields,

$$y(k+1) = r(k)\, y(k) + u(k), \tag{5}$$

where

$$u(k) = M_{an}(k) - \lambda_d M_{fn}(k). \tag{6}$$

Next, the detailed design process of the stochastic MPC algorithm will be given:

Step 1. Prediction of $y(k)$ and $u(k)$: For system (5), the error of regulation of the air-fuel ratio $y(k)$ and the residual gas fraction $r(k)$ are available at sampling point k by estimation [21]. Based on $y(k)$ and $r(k)$, the future error of regulation of the air-fuel ratio and the future fresh fuel mass trajectories can be expressed as

$$\begin{aligned} &y(k+1/k, r(k+1/k)), y(k+2/k, r(k+2/k)), \\ &\quad \cdots, y(k+N_p-1/k, r(k+N_p-1/k)), \end{aligned} \tag{7}$$

$$\begin{aligned} &u(k), u(k+1/k, r(k+1/k)), \\ &\quad \cdots, u(k+N_c-1/k, r(k+N_c-1/k)), \\ &\quad \cdots, u\left(k+N_p-1/k, r(k+N_p-1/k)\right), \end{aligned} \tag{8}$$

where N_p and N_c denote the corresponding horizons, and

$$\begin{aligned} &u(k+N_c-1/k, r(k+N_c-1/k)) \\ &\quad = u(k+N_c/k, r(k+N_c/k)) \\ &\quad = \cdots = u\left(k+N_p-1/k, r(k+N_p-1/k)\right). \end{aligned} \tag{9}$$

Based on (5) and the future fresh fuel mass trajectories (8), the future error of regulation of the air-fuel ratio can be expressed as follows:

$$\begin{aligned} &y(k+2/k, r(k+2/k)) \\ &= \sum_{j=1}^{N_r} p_{ij} s_j y(k+1/k) + u(k+1/k, r(k+1/k)) \\ &= \sum_{j=1}^{N_r} p_{ij} s_j s_i y(k) + \sum_{j=1}^{N_r} p_{ij} s_j u(k) \\ &\quad + u(k+1/k, r(k+1/k)), \end{aligned}$$

$$
\begin{aligned}
&\vdots\\
&y\left(k+N_p/k, r(k+N_p/k)\right)\\
&=\Omega_{y(k)}s_i y\left(k\right)+\Omega_{u(k)}u\left(k\right)\\
&\quad+\cdots+\Omega_{u(k+N_c-1)}u\left(k+N_c-1/k, r(k+N_c-1/k)\right)\\
&\quad+\cdots+\Omega_{u(k+N_p-2)}u\left(k+N_p-2/k, r(k+N_p-2/k)\right)\\
&\quad+u\left(k+N_p-1/k, r(k+N_p-1/k)\right), \qquad (10)
\end{aligned}
$$

where

$$
\begin{aligned}
\Omega_{y(k)} &= \left(\sum_{v=1}^{N_r}\sum_{l=1}^{N_r}p_{vl}s_l\right)^{N_p-2}\sum_{j=1}^{N_r}p_{ij}s_j,\\
\Omega_{u(k)} &= \left(\sum_{v=1}^{N_r}\sum_{l=1}^{N_r}p_{vl}s_l\right)^{N_p-2}\sum_{j=1}^{N_r}p_{ij}s_j,\\
&\vdots\\
\Omega_{u(k+N_c-1)} &= \left(\sum_{v=1}^{N_r}\sum_{l=1}^{N_r}p_{vl}s_l\right)^{N_p-N_c},\\
&\vdots\\
\Omega_{u(k+N_p-2)} &= \sum_{v=1}^{N_r}\sum_{l=1}^{N_r}p_{vl}s_l. \qquad (11)
\end{aligned}
$$

Step 2. Optimization within the horizon N_p: Let $J(y\left(k\right), r\left(k\right), u_{[k,k+N_p-1]/k})$ denotes the cost function as follows:

$$
\begin{aligned}
&J(y\left(k\right), r\left(k\right), u_{[k,k+N_p-1]/k})\\
&=E\left\{\sum_{n=0}^{N_p-1}\left[Q(k+n/k, r(k+n/k))y^2(k+n/k, r(k+n/k))\right.\right.\\
&\quad+R(k+n/k, r(k+n/k))u^2(k+n/k, r(k+n/k))]\\
&\quad+\Omega(k+N_p/k, r(k+N_p/k))y^2(k+N_p/k, r(k\\
&\quad\left.\left.+N_p/k))\right\}, \qquad (12)
\end{aligned}
$$

where $Q(k+n/k, r(k+n/k))>0, R(k+n/k, r(k+n/k))>0, \infty>\Omega(k+n/k, r(k+N_p/k))>0$, and N_p is a finite positive integer. Define

$$
\begin{aligned}
&V\left(y\left(k\right), r\left(k\right)=s_i\right)\\
&=J(y\left(k\right), r\left(k\right), u^*_{[k,k+N_p-1]/k})\\
&=\min E\left\{\sum_{n=0}^{N_p-1}\left[Q(k+n/k, r(k+n/k))y^2(k+n/k,\right.\right.\\
&\quad r(k+n/k))+R(k+n/k, r(k+n/k))u^2(k+n/k,\\
&\quad r(k+n/k))]+\Omega(k+N_p/k, r(k+N_p/k))y^2(k+N_p/k,\\
&\quad\left.\left.r(k+N_p/k))/r(k)=s_i\right\} \qquad (13)
\end{aligned}
$$

where $u^*_{[k,k+N_p-1]/k}$ is the optimal control sequence. Using the optimality principle, we have

$$
\begin{aligned}
&V\left(y\left(k\right), r\left(k\right)=s_i\right)\\
&\quad=\min E\left\{Q\left(k, s_i\right)y^2\left(k\right)+R(k, s_i)u^2(k)\right.\\
&\qquad\left.+V\left(y\left(k+1\right), r\left(k+1\right)=s_j\right)/r(k)=s_i\right\}. \qquad (14)
\end{aligned}
$$

Choose

$$
V\left(y\left(k\right), r\left(k\right)=s_i\right)=\alpha\left(k, s_i\right)y^2\left(k\right), \qquad (15)
$$

where $\alpha\left(k, s_i\right)>0$ satisfies

$$
\alpha\left(k+n_p/k, s_i\right)=\Omega(k+n_p/k, s_i). \qquad (16)
$$

Substituting (5) and (15) into (14), we can obtain

$$
\begin{aligned}
&\alpha\left(k, s_i\right)y^2\left(k\right)\\
&=\min E\left\{Q\left(k, s_i\right)y^2\left(k\right)+R(k, s_i)u^2(k)\right.\\
&\quad\left.+\alpha\left(k+1, r\left(k+1\right)=s_j/r(k)=s_i\right)\left(s_i y\left(k\right)+u\left(k\right)\right)^2\right\}\\
&=\min\left\{Q\left(k, s_i\right)y^2\left(k\right)+R(k, s_i)u^2(k)\right.\\
&\quad\left.+\alpha\left(k+1, s_j\right)p_{ij}(s_i y\left(k\right)+u\left(k\right))^2\right\}. \qquad (17)
\end{aligned}
$$

Based on the first derivative of (17) with respect to $u(k)$, the optimal control can be obtained as follows:

$$
u^*\left(k\right)=-\frac{\alpha\left(k+1, s_j\right)p_{ij}s_i}{R\left(k, s_i\right)+\alpha\left(k+1, s_j\right)p_{ij}}y\left(k\right). \qquad (18)
$$

Considering (17) and (18), we obtain

$$
\begin{aligned}
&\alpha\left(k, s_i\right)\\
&=Q\left(k, s_i\right)+\frac{R(k, s_i)\alpha^2\left(k+1, s_j\right)p_{ij}^2s_i^2}{\left(R\left(k, s_i\right)+\alpha\left(k+1, s_j\right)p_{ij}\right)^2}\\
&\quad+\alpha\left(k+1, s_j\right)p_{ij}\left(s_i-\frac{\alpha\left(k+1, s_j\right)p_{ij}s_i}{R\left(k, s_i\right)+\alpha\left(k+1, s_j\right)p_{ij}}\right)^2. \qquad (19)
\end{aligned}
$$

Based on (6), the optimal fresh fuel mass $M^*_{fn}\left(k\right)$ can be obtained as follows:

$$
M^*_{fn}\left(k\right)=\frac{M_{an}(k)}{\lambda_d}+\frac{\alpha\left(k+1, s_j\right)p_{ij}s_i y(k)}{\lambda_d\left(R\left(k, s_i\right)+\alpha\left(k+1, s_j\right)p_{ij}\right)}. \qquad (20)
$$

Step 3. At sampling point $k+1$, $M^*_{fn}\left(k+1\right)$ can be obtained by repeating step 1 and step 2.

Remark 1: The traditional control approaches, which usually employ the robust control method to address the mode transitions of a discrete-time system with jump parameters, do not take into account the statistical information of the mode transitions. To solve this problem, the mode transitions are modeled as a Markov chain, and the statistical information of the mode transitions is fully considered in the corresponding stochastic control algorithm. However, the control performance of the stochastic control algorithm is considerably influenced by the accuracy of the system model. In general,

the proposed stochastic MPC exhibits a better control performance than that of the above mentioned control approach, as the statistical information of the mode transitions is fully utilized, and the accuracy of the system model does not have a strict requirement due to its receding horizon implementation mechanism. It is noted that the better control performance is usually achieved at the cost of increased online computational burden. However, with the improvement in the computational capabilities, the computational issues of the MPC are being gradually alleviated.

Remark 2: The optimal controller (18) at sampling point k is obtained by deriving (17) with respect to $u(k)$ based on the optimality principle, and makes the cost function (12) reach the minimum value within the horizon N_p.

III. STABILITY ANALYSIS

This section discusses the stabilization of the closed-loop system consisting of (5), (18) and (19). Consider a system with the following discrete-time form:

$$\begin{aligned} x(k+1) &= A(r(k))x(k) \\ x(0) &= x_0, \quad r(0) = r_0, \end{aligned} \tag{21}$$

where $x(k)$ denotes the system state, $r(k)$ denotes a finite state aperiodic irreducible Markov chain, and $x(0)$ and $r(0)$ denote the corresponding initial values.

Definition 1 [22]: If for every initial values $x(0)$ and $r(0)$, a finite bound $M(x(0), r(0))$ exists, such that:

$$\lim_{N\to\infty} E\left\{\sum_{k=0}^{N} x^T(k)\,x(k)\,|x(0), r(0)\right\} < M(x(0), r(0)), \tag{22}$$

system (21) is considered stochastically stable. Moreover, (21) implies that

$$\lim_{N\to\infty} E\left\{x^T(k)\,x(k)\,|x(0), r(0)\right\} \to 0. \tag{23}$$

Lemma 1 [22]: If given a set of symmetric matrices $\{W(s_i) > 0, i = 1, \cdots, N\}$, and a set of appropriate dimension matrices $\{\chi(s_i) > 0, i = 1, \cdots, N\}$ satisfies

$$\sum_{j=1}^{N} p_{ij} A^T(s_i)\chi(s_j)A(s_i) - \chi(s_i) = -W(s_i), \tag{24}$$

system (21) is stochastically stable.

Proposition 1 for every $r(k+N_p/k) = s_i$ and all $k \in [0, \infty)$, the terminal weighting number $\Omega(k+N_p/k, s_j)$ satisfies

$$\begin{aligned} &\Omega(k+N_p/k, s_i) \\ &\geq Q\left(k+N_p/k, s_i\right) \\ &\quad + \frac{R\left(k+N_p/k, s_i\right)\alpha^2\left(k+N_p+1/k, s_j\right)p_{ij}^2 s_i^2}{\left(R\left(k+N_p/k, s_i\right)+\alpha\left(k+N_p+1/k, s_j\right)p_{ij}\right)^2} \\ &\quad + \Omega(k+N_p+1/k, s_j)p_{ij} \\ &\quad \times \left(s_i - \frac{\alpha\left(k+N_p+1/k, s_j\right)p_{ij}s_i}{R \times \left(k+N_p/k, s_i\right)+\alpha\left(k+N_p+1/k, s_j\right)p_{ij}}\right)^2. \end{aligned} \tag{25}$$

In this case, the closed-loop system consisting of (5), (18) and (19) is stochastically stable.

Proof: From (10), we have

$$\begin{aligned} &V\left(y(k+1), r(k+1) = s_j / r(k) = s_i\right) - V(y(k), s_i) \\ &= \min E\left\{\sum_{n=0}^{N_p}[Q(k+n/k, r(k+n/k))y^2(k+n/k, r(k+n/k)) \right. \\ &\quad + R(k+n/k, r(k+n/k))u^2(k+n/k, r(k+n/k))] \\ &\quad + \Omega(k+N_p+1/k, r(k+N_p+1/k))y^2(k+N_p+1/k, \\ &\quad \left. r(k+N_p+1/k))/r(k) = s_i\right\} \\ &\quad - \min E\left\{\sum_{n=0}^{N_p-1}[Q(k+n/k, r(k+n/k))y^2(k+n/k, \right. \\ &\quad r(k+n/k)) + R(k+n/k, r(k+n/k))u^2(k+n/k, \\ &\quad r(k+n/k))] + \Omega(k+N_p/k, r(k+N_p/k))y^2(k+N_p/k, \\ &\quad \left. r(k+N_p/k))/r(k) = s_i\right\}. \end{aligned} \tag{26}$$

Rearranging (26) yields,

$$\begin{aligned} &V\left(y(k+1), r(k+1) = s_j / r(k) = s_i\right) - V(y(k), s_i) \\ &= Q(k+N_p/k, s_i)y^2(k+N_p/k, s_i) \\ &\quad + R(k+N_p/k, s_i)u^2(k+N_p/k, s_i) \\ &\quad + \Omega(k+N_p+1/k, s_j)p_{ij}(s_i y(k+N_p/k, s_i) \\ &\quad + u(k+N_p/k, s_i))^2 - \Omega(k+N_p/k, s_i)y^2(k+N_p/k, s_i). \end{aligned} \tag{27}$$

Considering (18) and (27), we can obtain

$$V\left(y(k+1), r(k+1) = s_j / r(k) = s_i\right) - V(y(k), s_i) \leq 0. \tag{28}$$

Lemma 1 indicates that, the closed-loop system involving (5), (17) and (18) is stochastically stable.

IV. NUMERICAL SIMULATION

The effectiveness of the designed stochastic MPC regulator is demonstrated in this section. The numerical simulation which is performed on the Matlab/Simulink platform, involves the dynamic equations of the air and fuel paths (1) and models in mean value form [23]–[25], as follows:

$$\begin{aligned} y(k) &= M_a(k) - M_f(k)\lambda_d, \\ M_a(k+1) &= \left(M_a(k) - \lambda_d \mu M_f(k)\right) r(k) + M_{an}(k), \\ M_f(k+1) &= M_f(k)(1-\mu)\, r(k) + M_{fn}(k), \\ \dot{M}_{an} &= \frac{\rho_a V_d \eta_v}{4\pi P_a}\omega_e P_m, \\ T_e &= \frac{H_u V_d \eta_i \eta_v P_m}{4\pi R T_m \lambda}, \\ J\dot{\omega}_e &= T_e - T_l, \end{aligned}$$

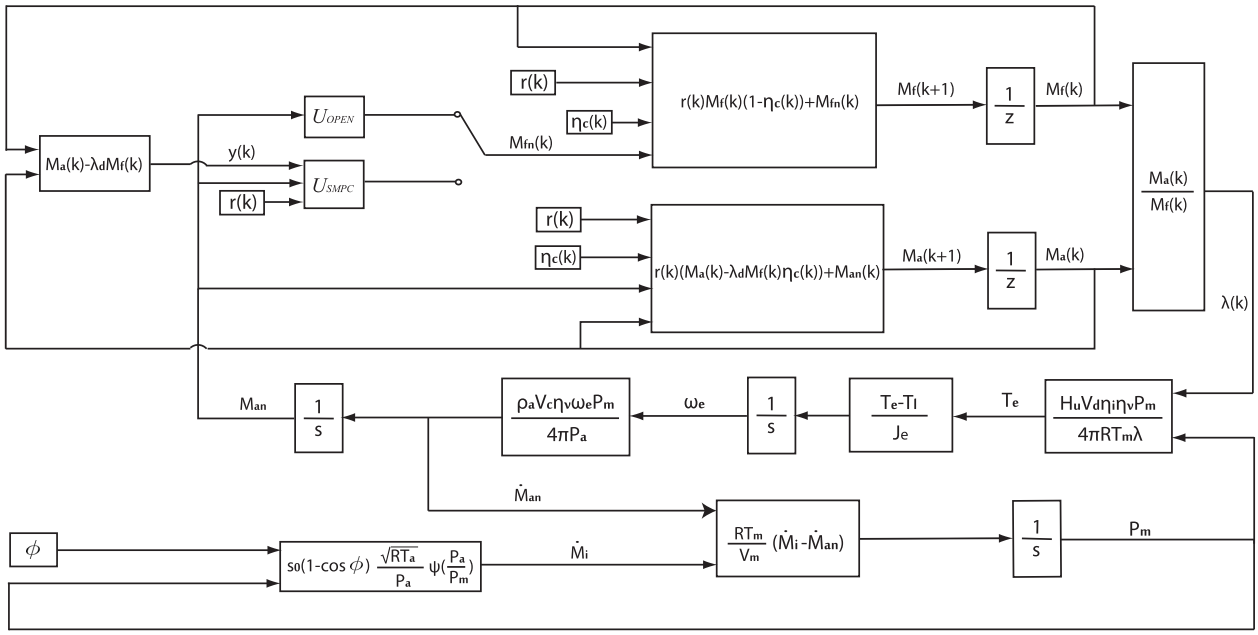

FIGURE 1. Schematic of the numerical simulation control structure.

$$\dot{P}_m = \frac{RT_m}{V_m}\left(\dot{M}_i - \dot{M}_{an}\right),$$
$$\dot{M}_i = s_0\left(1-\cos\phi\right)\frac{P_a}{\sqrt{RT_a}}\psi\left(\frac{P_a}{P_m}\right), \tag{29}$$

where T_m is 298.15K, V_m is 5.897E-03m^3, V_d is 5.76E-04m^3, s_0 is 3.5E-03m^2, T_a is 298.15K, and

$$\psi(s) = \begin{cases} s^{\frac{2}{k}}\left(\frac{2k}{k-1}(1-s)\right)^{\frac{k-1}{k}} & if\ s \geq \left(\frac{2}{k+1}\right)^{\frac{k}{k-1}} \\ k\left(\frac{2}{k+1}\right)^{\frac{k+1}{k-1}} & if\ otherwise. \end{cases} \tag{30}$$

The numerical simulation control structure diagram is shown in Fig. 1. The simulation parameters corresponding to two working conditions W_1 and W_2 are as follows. In W_1, the engine revolution is 1200rpm, external burden is 60Nm, and ideal air-fuel ratio is 17.4. In W_2, the engine revolution is 1600rpm, external burden is 90Nm, and ideal air-fuel ratio is 17.4. For the two working conditions, N_p and N_c are 10 and 5, respectively. The state spaces and one-step transition probability matrices of W_1 and W_2 are as follows:

$$S_{W_1} = \{0.085, 0.082, 0.080, 0.076\}, \tag{31}$$
$$S_{W_2} = \{0.087, 0.081, 0.075, 0.072\}, \tag{32}$$
$$P_{W_1} = \begin{pmatrix} 0.10 & 0.33 & 0.39 & 0.27 \\ 0.11 & 0.14 & 0.39 & 0.36 \\ 0.31 & 0.14 & 0.14 & 0.41 \\ 0.41 & 0.31 & 0.10 & 0.18 \end{pmatrix}, \tag{33}$$
$$P_{W_2} = \begin{pmatrix} 0.25 & 0.02 & 0.19 & 0.54 \\ 0.51 & 0.24 & 0.04 & 0.21 \\ 0.21 & 0.52 & 0.23 & 0.04 \\ 0.03 & 0.21 & 0.55 & 0.21 \end{pmatrix}. \tag{34}$$

By setting $Q(k+n/k, r(k+n/k))$ and $R(k+n/k, r(k+n/k))$ as 1 for all $k \in [0, \infty)$ and $n \in [0, n_p]$, the values of $\alpha(k+n/k, s_i)$ for working conditions W_1 and W_2 can be obtained as follows:

$$\alpha_{W_1}(k+n/k, s_i) = \begin{cases} 1.00127, & if\ s_i = 0.085 \\ 1.00118, & if\ s_i = 0.082 \\ 1.00112, & if\ s_i = 0.08 \\ 1.00101, & if\ s_i = 0.076, \end{cases} \tag{35}$$

and

$$\alpha_{W_2}(k+n/k, s_i) = \begin{cases} 1.00133, & if\ s_i = 0.087 \\ 1.00115, & if\ s_i = 0.081 \\ 1.00099, & if\ s_i = 0.075 \\ 1.00091, & if\ s_i = 0.072. \end{cases} \tag{36}$$

Considering (31)-(36), for every $s_i \in S$, we choose

$$\Omega(k+N_p-1/k, s_i) = 1.6 + 0.25\Omega(k+N_p/k, s_j)$$
$$\Omega(k+10/k, s_j) = 1. \tag{37}$$

In this case, (25) is satisfied. The air-fuel ratio and fresh fuel mass samples under W_1 and W_2 are exhibited in Figs. 2-5, where U_{SMPC} denotes the designed stochastic MPC algorithm, and the open-loop controller U_{OPEN} is defined as follows:

$$U_{OPEN} = \frac{M_{an}(k)}{\lambda_d}. \tag{38}$$

Fig. 2 and Fig. 4 indicate that the air-fuel ratio can be regulated into a neighborhood of its ideal value by using both U_{SMPC} and U_{OPEN}, and the fluctuation range of the air-fuel ratio of U_{SMPC} is smaller than that of U_{OPEN} under

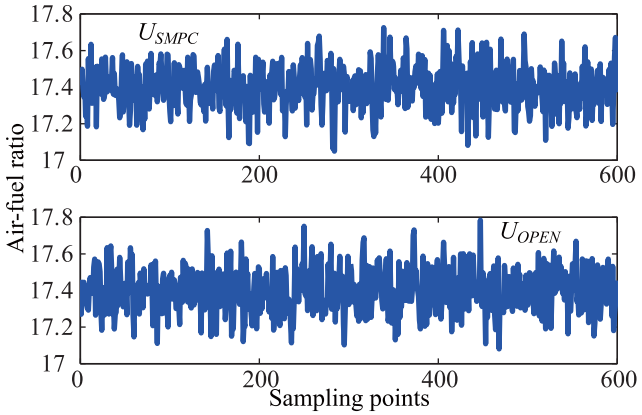

FIGURE 2. Control performances of air-fuel ratio of W_1.

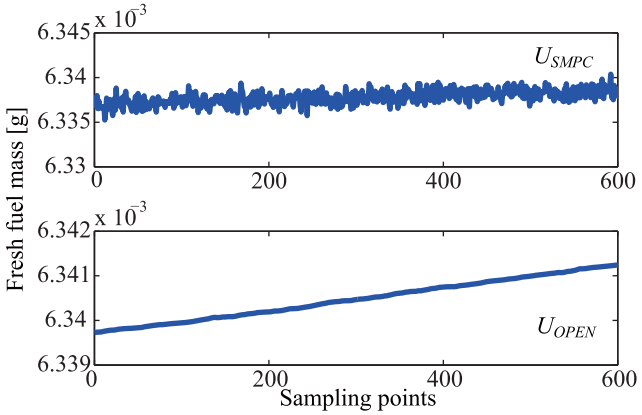

FIGURE 3. Fresh fuel masses of W_1.

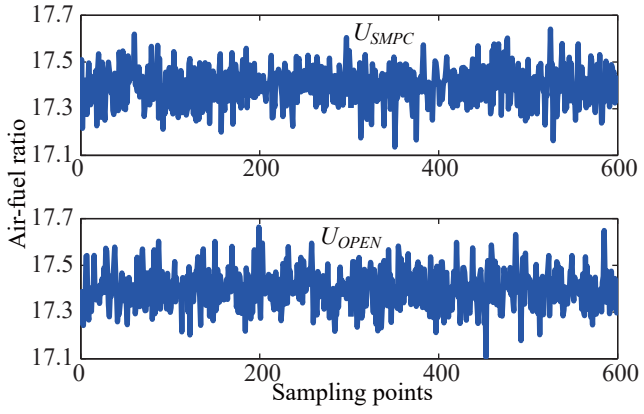

FIGURE 4. Control performances of air-fuel ratio of W_2.

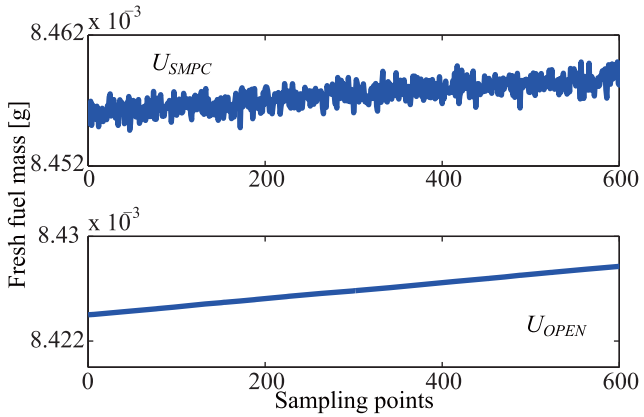

FIGURE 5. Fresh fuel masses of W_2.

W_1 and W_2. In contrast, the fluctuation range of the fresh fuel mass of U_{SMPC} is larger than that of U_{OPEN} under W_1 and W_2, which can be observed from Fig. 3 and Fig. 5. To enable the quantitative examination of the control performances of U_{SMPC} and U_{OPEN}, the cost function J of W_1 and W_2 are listed in Table 1, where

$$J = \sum_{k=1}^{N} \left\{ (\lambda(k) - \lambda_d)^2 + u^2(k) \right\},$$
$$\varepsilon = \frac{\left| J_{U_{SMPC}} - J_{U_{OPEN}} \right|}{J_{U_{SMPC}}}. \tag{39}$$

The values of the controllers U_{SMPC} and U_{OPEN} listed in Table 1 indicated that the cost function of U_{SMPC} is smaller than that of U_{OPEN}, and the values of ε for W_1 and W_2 are 0.503% and 0.644%, respectively. Therefore, the proposed stochastic MPC algorithm U_{SMPC} exhibits a better performance under working conditions W_1 and W_2.

Remark 3: The mean value models reported in references [23], [24] and [25] contain the dynamic equations of the air mass flow leaving the manifold into the cylinders, torque generated, pressure in the manifold and air mass flow passing through the throttle, these equations, along with (1), constitute the dynamic model of the CNG engines.

TABLE 1. Cost functions of W_1 and W_2.

	$J_{U_{SMPC}}$	$J_{U_{OPEN}}$	ε
W_1	23.5608	23.6793	0.503%
W_2	20.3094	20.4443	0.644%

V. CONCLUSION

This paper proposes a stochastic MPC regulator based on a dynamic model of CNG engines in the discrete-time form, which contains the air path and fuel path dynamics. The whole system is deduced to be stochastically stable. The effectiveness of the designed stochastic MPC regulator is demonstrated by performing a numerical simulation. The control performance of the proposed stochastic MPC depends on the computer performance since the online computational burden is augmented in this technique. The limitations of the increase in the computational burden are being progressively overcome via improvements of the computer performance. An on-line technique to estimate the masses of the total air and the total fuel in-cylinder should be designed, as these values can't be directly estimated. Furthermore, the control accuracy of the air-fuel ratio of CNG engines is affected by estimation errors. As an effective control algorithm, the

stochastic MPC has been applied to the energy distribution of hybrid electrical vehicles, coordinated dispatch of power grid and other applications.

REFERENCES

[1] S. Pischinger, M. Umierski, and B. Hüchtebrock, "New CNG concepts for passenger cars: High torque engines with superior fuel consumption," SAE Paper 2003-01-2264, 2003.
[2] M. D. Ruter, D. B. Olsen, M. V. Scotto, and M. A. Perna, "NOx reduction from a large bore natural gas engine via reformed natural gas prechamber fueling optimization," *Fuel*, vol. 91, no. 1, pp. 298–306, Jan. 2012.
[3] J. Zhao, F. Ma, X. Xiong, J. Deng, L. Wang, N. Naeve, and S. Zhao, "Effects of compression ratio on the combustion and emission of a hydrogen enriched natural gas engine under different excess air ratio," *Energy*, vol. 59, pp. 658–665, Sep. 2013.
[4] A.-H. Kakaee, A. Paykani, and M. Ghajar, "The influence of fuel composition on the combustion and emission characteristics of natural gas fueled engines," *Renew. Sustain. Energy Rev.*, vol. 38, pp. 64–78, Oct. 2014.
[5] J. Alanen, E. Saukko, K. Lehtoranta, T. Murtonen, H. Timonen, R. Hillamo, P. Karjalainen, H. Kuuluvainen, J. Harra, J. Keskinen, and T. Rönkkö, "The formation and physical properties of the particle emissions from a natural gas engine," *Fuel*, vol. 162, pp. 155–161, Dec. 2015.
[6] L.-P. Yang, E.-Z. Song, S.-L. Ding, R. J. Brown, N. Marwan, and X.-Z. Ma, "Analysis of the dynamic characteristics of combustion instabilities in a pre-mixed lean-burn natural gas engine," *Appl. Energy*, vol. 183, pp. 746–759, Dec. 2016.
[7] B. Yan, H. Wang, Z. Zheng, Y. Qin, and M. Yao, "The effects of LIVC miller cycle on the combustion characteristics and thermal efficiency in a stoichiometric operation natural gas engine with EGR," *Appl. Thermal Eng.*, vol. 122, pp. 439–450, Jul. 2017.
[8] D. K. Srivastava and A. K. Agarwal, "Combustion characteristics of a variable compression ratio laser-plasma ignited compressed natural gas engine," *Fuel*, vol. 214, pp. 322–329, Feb. 2018.
[9] F. Yan, L. Xu, and Y. Wang, "Application of hydrogen enriched natural gas in spark ignition IC engines: From fundamental fuel properties to engine performances and emissions," *Renew. Sustain. Energy Rev.*, vol. 82, pp. 1457–1488, Feb. 2018.
[10] M. Garg and R. V. Ravikrishna, "In-cylinder flow and combustion modeling of a CNG-fuelled stratified charge engine," *Appl. Thermal Eng.*, vol. 149, pp. 425–438, Feb. 2019.
[11] J. Yang and F. Y. Yi, "Adaptive fuel-air ratio control of compressed natural gas engines," *Proc. 38th Chin. Control Conf.*, Guangzhou, China, vol. 30, Jul. 2019, pp. 6470–6474.
[12] R. Tiwari and S. Janardhanan, "DSP based tracking of twin spool gas turbine using reduced output feedback sliding mode control," in *Proc. 12th Int. Workshop Variable Struct. Syst.*, Mumbai, India, Jan. 2012, pp. 52–56.
[13] L. Fang, L. Ma, S. Ding, and D. Zhao, "Finite-time stabilization for a class of high-order stochastic nonlinear systems with an output constraint," *Appl. Math. Comput.*, vol. 358, pp. 63–79, Oct. 2019.
[14] S. Lee, C. Kim, S. Lee, J. Lee, and J. Kim, "Diesel injector nozzle optimization for high CNG substitution in a dual-fuel heavy-duty diesel engine," *Fuel*, vol. 262, Feb. 2020, Art. no. 116607.
[15] S. Di Cairano, D. Bernardini, A. Bemporad, and I. V. Kolmanovsky, "Stochastic MPC with learning for driver-predictive vehicle control and its application to HEV energy management," *IEEE Trans. Control Syst. Technol.*, vol. 22, no. 3, pp. 1018–1031, May 2014.
[16] X. Zeng and J. Wang, "A parallel hybrid electric vehicle energy management strategy using stochastic model predictive control with road grade preview," *IEEE Trans. Control Syst. Technol.*, vol. 23, no. 6, pp. 2416–2423, Nov. 2015.
[17] P. Kou, D. Liang, L. Gao, and F. Gao, "Stochastic coordination of plug-in electric vehicles and wind turbines in microgrid: A model predictive control approach," *IEEE Trans. Smart Grid*, vol. 7, no. 3, pp. 1537–1551, May 2016.
[18] M. Lorenzen, F. Dabbene, R. Tempo, and F. Allgower, "Constraint-tightening and stability in stochastic model predictive control," *IEEE Trans. Autom. Control*, vol. 62, no. 7, pp. 3165–3177, Jul. 2017.
[19] R. Kumar, M. J. Wenzel, M. J. Ellis, M. N. ElBsat, K. H. Drees, and V. M. Zavala, "A stochastic model predictive control framework for stationary battery systems," *IEEE Trans. Power Syst.*, vol. 33, no. 4, pp. 4397–4406, Jul. 2018.
[20] S. Raimondi Cominesi, M. Farina, L. Giulioni, B. Picasso, and R. Scattolini, "A two-layer stochastic model predictive control scheme for microgrids," *IEEE Trans. Control Syst. Technol.*, vol. 26, no. 1, pp. 1–13, Jan. 2018.
[21] J. Yang, T. Shen, and X. Jiao, "Model-based stochastic optimal air–fuel ratio control with residual gas fraction of spark ignition engines," *IEEE Trans. Control Syst. Technol.*, vol. 22, no. 3, pp. 896–910, May 2014.
[22] Y. Ji and H. J. Chizeck, "Jump linear quadratic Gaussian control: Steady state solution and testable conditions," *Control Theory Adv. Technol.*, vol. 6, no. 3, pp. 283–319, 1990.
[23] J. B. Heywood, *Internal Combustion Engine Fundamentals*. New York, NY, USA: McGraw-Hill, 1988.
[24] A. Stotsky, B. Egardt, and S. Eriksson, "Variable structure control of engine idle speed with estimation of unmeasurable disturbances," *J. Dyn. Syst., Meas., Control*, vol. 122, no. 4, pp. 599–603, Feb. 2000.
[25] E. Hendricks and S. C. Sorenson, "Mean value modeling of spark ignition engines," SAE Paper 900616, 1990.

JUN YANG received the Ph.D. degree from the Department of Electrical Engineering, Yanshan University, in 2014. In 2015, he joined Shandong Jiaotong University, where he is currently an Associate Professor with the School of Automotive Engineering. Since 2018, he has been a Postdoctoral Fellow of the School of Control Science and Engineering with Shandong University. His research interests include stochastic system control and engine control.

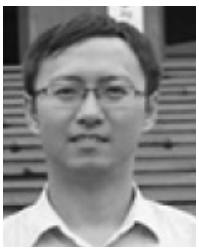

BO SUN received the B.S. and Ph.D. degrees from Shandong University, China, in 2004 and 2009, respectively. In 2010, he joined Shandong University, where he is currently an Associate Professor with the School of Control Science and Engineering. His current research interests include optimal control of engineering and combined cooling, and heating and power systems.